

Cite this: *Chem. Sci.*, 2018, 9, 5600

Thermodynamic *versus* kinetic control in substituent redistribution reactions of silylium ions steered by the counteranion†

Lukas Omann, ^a Bimal Pudasaini, ^b Elisabeth Irran, ^{‡a} Hendrik F. T. Klare, ^a Mu-Hyun Baik ^{*bc} and Martin Oestreich ^{*a}

An in-depth experimental and theoretical study of the substituent exchange reaction of silylium ions is presented. Apart from the substitution pattern at the silicon atom, the selectivity of this process is predominantly influenced by the counteranion, which is introduced with the trityl salt in the silylium ion generation. In contrast to Müller's protocol for the synthesis of triarylsilylium ions under kinetic control, the use of Reed's carborane anions leads to contact ion pairs, allowing selective formation of trialkylsilylium ions under thermodynamic control. DFT calculations finally revealed an unexpected mechanism for the rate-determining alkyl exchange step, which is initiated by an unusual 1,2-silyl migration in the intermediate *ipso*-disilylated arenium ion. The resulting *ortho*-disilylated arenium ion can then undergo an alkyl transfer *via* a low-barrier five-centered transition state.

Received 22nd April 2018
Accepted 20th May 2018

DOI: 10.1039/c8sc01833b

rsc.li/chemical-science

Introduction

Silylium ions (R_3Si^+) have recently emerged as useful and versatile catalysts for synthetically attractive transformations.^{1,2} The most commonly used approach to generate silylium ions is the Bartlett–Condon–Schneider reaction,³ that is the silicon-to-carbon hydride transfer from a hydrosilane to the trityl cation (Ph_3C^+) paired with a weakly coordinating counteranion.^{4,5} However, substituent redistribution of the hydrosilane starting material can occur under these highly Lewis acidic reaction conditions, leading to undesired mixtures of various silicon compounds.^{6–8} Hence, hydrosilanes containing three identical substituents, *e.g.* Et_3SiH or iPr_3SiH , are usually employed in this reaction.⁹ Conversely, Müller and co-workers have turned this unselective process into a useful synthetic route to triarylsilylium ions (Scheme 1, top).¹⁰ When sterically demanding methyl(diaryl)silanes $MeAr_2SiH$ are used in the hydride abstraction with $Ph_3C^+[B(C_6F_5)_4]^-$, the formation of otherwise difficult to prepare triarylsilylium ions $Ar_3Si^+[B(C_6F_5)_4]^-$ is

observed.¹¹ Notably, the use of less bulky hydrosilanes such as $MePh_2SiH$ or $Me(o-Tol)_2SiH$ does not give triarylsilylium ions but mixtures of different silicon cations.¹²

Herein, we report that treatment of hydrosilanes of type Me_2RSiH ($R = aryl, benzyl$) with Reed's carborane-based trityl salt $Ph_3C^+[CHB_{11}H_5Br_6]^-$ (ref. 13) results in substituent exchange reactions selectively forming the elusive trimethylsilylium ion $Me_3Si^+[CHB_{11}H_5Br_6]^-$ (Scheme 1, bottom). This method thus complements Müller's approach and offers a practical route to Me_3Si^+ , avoiding the use of gaseous and highly flammable Me_3SiH .¹⁴ A systematic experimental and computational investigation was performed to gain a full

^aInstitut für Chemie, Technische Universität Berlin, Strasse des 17. Juni 115, 10623 Berlin, Germany. E-mail: martin.oestreich@tu-berlin.de

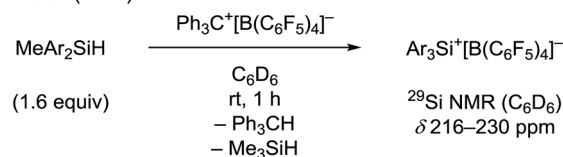
^bCenter for Catalytic Hydrocarbon Functionalizations, Institute for Basic Science (IBS), Daejeon, 34141, Republic of Korea

^cDepartment of Chemistry, Korea Advanced Institute of Science and Technology (KAIST), Daejeon, 34141, Republic of Korea. E-mail: mbaik2805@kaist.ac.kr

† Electronic supplementary information (ESI) available: Experimental details, characterization, spectroscopic and crystallographic data, DFT calculation methods, energy data, and the coordinates of the calculated geometries. CCDC 1818576, 1818581, and 1818582. For ESI and crystallographic data in CIF or other electronic format see DOI: 10.1039/c8sc01833b

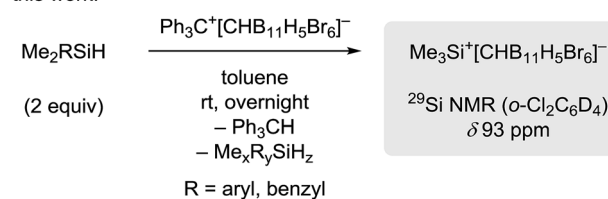
‡ Responsible for X-ray diffraction analysis.

Müller (2011):



Ar = 2,6-disubstituted phenyl

this work:



Scheme 1 Divergence in the generation of silylium ions by substituent redistribution ($x + y + z = 4$).



mechanistic picture of this phenomenon. DFT calculations revealed an unexpected mechanism and suggested an active role of the carborane counteranion in the outcome of these reactions.

Results and discussion

Generation of the trimethylsilylium ion by substituent redistribution

When a mixture of Me_2PhSiH and $\text{Ph}_3\text{C}^+[\text{CHB}_{11}\text{H}_5\text{Br}_6]^-$ in toluene was stirred overnight at room temperature, a white suspension was obtained. The solid was collected by filtration, washed with *n*-pentane, and dissolved in *o*- $\text{Cl}_2\text{C}_6\text{D}_4$ for NMR spectroscopic analysis. Unexpectedly, only a singlet at 0.83 ppm was detected in the ^1H NMR spectrum, while no aromatic resonances except for those of the deuterated solvent were observed. The low-field ^{29}Si NMR chemical shift of 93 ppm in the corresponding $^1\text{H}/^{29}\text{Si}$ HMQC spectrum, which is characteristic of trialkylsilylium ions, indicated clean formation of $\text{Me}_3\text{Si}^+[\text{CHB}_{11}\text{H}_5\text{Br}_6]^-$ (Fig. 1). The structural integrity of the carborane counteranion was confirmed by ^{11}B NMR spectroscopy.

Unambiguous evidence for the structure of $\text{Me}_3\text{Si}^+[\text{CHB}_{11}\text{H}_5\text{Br}_6]^-$ was eventually provided by its crystallographic characterization (Fig. 2).¹⁵ Single crystals suitable for X-ray diffraction analysis were obtained by vapor diffusion with *n*-hexane from a solution of the silylium salt in *o*- $\text{F}_2\text{C}_6\text{H}_4$ at room temperature. In accordance with reported molecular structures of silylium carboranes,¹⁶ one bromine atom at the pentagonal belt of the icosahedral anion is bound to the silicon cation. Both the Si–Br bond distance of 2.435(6) Å and the sum of all C–Si–C bond angles of 346.3(6)° are comparable to the larger $\text{Et}_3\text{Si}^+[\text{CHB}_{11}\text{H}_5\text{Br}_6]^-$.

In contrast to the clean formation of Me_3Si^+ , the non-polar *n*-pentane filtrate contained several tri- and tetraorganosilanes, such as Ph_4Si , MePh_3Si , Ph_3SiH , $\text{Me}_2\text{Ph}_2\text{Si}$, MePh_2SiH , Me_3PhSi , and Me_2PhSiH , as verified by GC-MS analysis. Since silylium

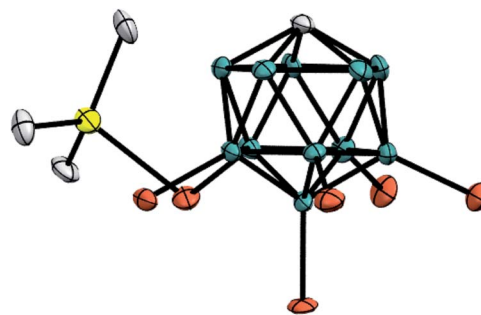


Fig. 2 Molecular structure of $\text{Me}_3\text{Si}^+[\text{CHB}_{11}\text{H}_5\text{Br}_6]^-$ (thermal ellipsoids at the 50% probability level; H atoms omitted for clarity).

ions are known to promote substituent redistribution,⁸ this result did not come as a surprise but raised the question why Me_3Si^+ was selectively formed in this reaction mixture, whereas Müller's conditions cleanly afford sterically congested triarylsilylium ions.¹⁰

Influence of the substituent pattern at the silicon atom on the selectivity of the substituent redistribution reaction

To understand the differences between Müller's protocol¹⁰ and our findings, we systematically studied the hydride transfer reaction of various hydrosilanes of type MeAr_2SiH and Me_2ArSiH using trityl salts $\text{Ph}_3\text{C}^+[\text{B}(\text{C}_6\text{F}_5)_4]^-$ and $\text{Ph}_3\text{C}^+[\text{CHB}_{11}\text{H}_5\text{Br}_6]^-$ (Table 1). Depending on the counteranion, slightly modified procedures were applied for the generation of the silicon cations (see the ESI† for details). For all reactions, an excess of hydrosilane (4 equiv.) was used, thereby

Table 1 Silylium ion generation by substituent redistribution: effect of the hydrosilane and counteranion (Si = triorganosilyl)

Entry ^a	Si–H (4 equiv.)	$[\text{X}]^-$	Si^+	$\delta(^{29}\text{Si})^b$ [ppm]
1	$\text{Me}(\text{C}_6\text{Me}_5)_2\text{SiH}$	$[\text{B}(\text{C}_6\text{F}_5)_4]^-$	$(\text{C}_6\text{Me}_5)_3\text{Si}^+$	217
2	$\text{Me}(\text{C}_6\text{Me}_5)_2\text{SiH}$	$[\text{CHB}_{11}\text{H}_5\text{Br}_6]^-$	$(\text{C}_6\text{Me}_5)_3\text{Si}^+$	217
3	MePh_2SiH	$[\text{B}(\text{C}_6\text{F}_5)_4]^-$	— ^c	—
4	MePh_2SiH	$[\text{CHB}_{11}\text{H}_5\text{Br}_6]^-$	MePh_2Si^+ / $\text{Me}_2\text{PhSi}^{+d}$	57/76
5	Me_2PhSiH	$[\text{B}(\text{C}_6\text{F}_5)_4]^-$	— ^c	—
6	Me_2PhSiH	$[\text{CHB}_{11}\text{H}_5\text{Br}_6]^-$	Me_3Si^+	93
7	$\text{Me}_2(\text{C}_6\text{Me}_5)\text{SiH}$	$[\text{B}(\text{C}_6\text{F}_5)_4]^-$	$(\text{C}_6\text{Me}_5)_3\text{Si}^+$	217
8 ^e	$\text{Me}_2(\text{C}_6\text{Me}_5)\text{SiH}$	$[\text{CHB}_{11}\text{H}_5\text{Br}_6]^-$	Me_3Si^+	93

^a All reactions were performed according to General Procedure (GP) 1 for $\text{X}^- = [\text{B}(\text{C}_6\text{F}_5)_4]^-$ (C_6D_6 , room temperature, 60 min) or GP 2 for $\text{X}^- = [\text{CHB}_{11}\text{H}_5\text{Br}_6]^-$ (toluene, room temperature, 18–24 h). See the ESI† for details. ^b Measured in *o*- $\text{Cl}_2\text{C}_6\text{D}_4$. ^c A complex mixture was obtained as a result of counteranion decomposition.¹⁷ ^d Ratio of 79 : 21 determined by ^1H NMR spectroscopy. ^e Reaction performed at 50 °C for 72 h.

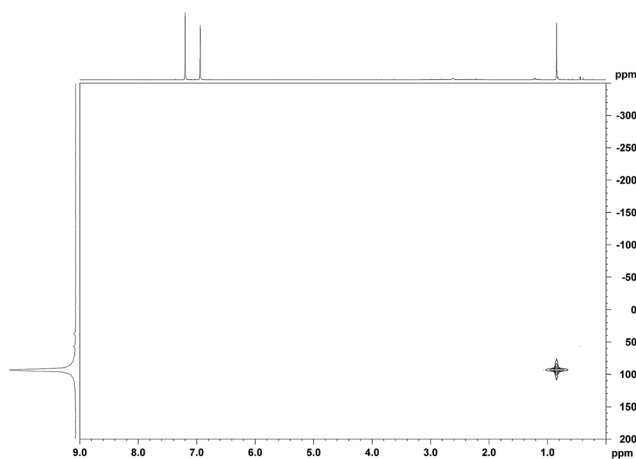


Fig. 1 $^1\text{H}/^{29}\text{Si}$ HMQC NMR spectrum (500/99 MHz, *o*- $\text{Cl}_2\text{C}_6\text{D}_4$, 298 K, optimized for $J = 7$ Hz) of $\text{Me}_3\text{Si}^+[\text{CHB}_{11}\text{H}_5\text{Br}_6]^-$ from the reaction of Me_2PhSiH with $\text{Ph}_3\text{C}^+[\text{CHB}_{11}\text{H}_5\text{Br}_6]^-$.



excluding any influence of stoichiometry on the product formation. In accordance with Müller's report, bulky methyl(diaryl)silane $\text{Me}(\text{C}_6\text{Me}_5)_2\text{SiH}$ was converted to the corresponding triarylsilylium ion, regardless of which counteranion was used (entries 1 and 2). In contrast, hydride abstraction from sterically less hindered MePh_2SiH with $\text{Ph}_3\text{C}^+[\text{B}(\text{C}_6\text{F}_5)_4]^-$ led to a complex reaction mixture as a result of anion decomposition (entry 3).^{12,17} The use of the carborane counteranion $[\text{CHB}_{11}\text{H}_5\text{Br}_6]^-$ furnished the unscrambled silylium ion $\text{MePh}_2\text{Si}^+[\text{CHB}_{11}\text{H}_5\text{Br}_6]^-$, as confirmed by X-ray diffraction analysis (entry 4; see the ESI† for the molecular structure of $\text{MePh}_2\text{Si}^+[\text{CHB}_{11}\text{H}_5\text{Br}_6]^-$).¹⁵ However, the formation of the MePh_2Si^+ cation was accompanied by a substantial amount of a second silylium ion, which was found to be the Me_2PhSi^+ cation.¹⁸ Notably, longer reaction times (7 days) or elevated temperatures ($50\text{ }^\circ\text{C}$ for 72 h) did not significantly change the product ratio of $\sim 79 : 21$ (not shown). In all cases, the generation of Me_3Si^+ was not observed. We then turned our attention to dimethyl(aryl)silanes (entries 5–8). The reaction of Me_2PhSiH with $\text{Ph}_3\text{C}^+[\text{B}(\text{C}_6\text{F}_5)_4]^-$ again resulted in decomposition of the borate counteranion (entry 5).¹⁷ Conversely, treatment of Me_2PhSiH with trityl carborane $\text{Ph}_3\text{C}^+[\text{CHB}_{11}\text{H}_5\text{Br}_6]^-$ exclusively afforded silylium salt $\text{Me}_2\text{PhSi}^+[\text{CHB}_{11}\text{H}_5\text{Br}_6]^-$ without detectable formation of MePh_2Si^+ or Me_2PhSi^+ (entry 6). Strikingly, hydride abstraction from sterically more demanding $\text{Me}_2(\text{C}_6\text{Me}_5)\text{SiH}$ led to the corresponding triarylsilylium ion in the presence of the borate counteranion (entry 7), while substituent redistribution into the ‘opposite direction’ was induced by the carborane anion,

now affording $\text{Me}_3\text{Si}^+[\text{CHB}_{11}\text{H}_5\text{Br}_6]^-$ (entry 8).¹⁹ However, heating of the reaction at $50\text{ }^\circ\text{C}$ for 72 h was necessary.

Overall, these results indicate that hydride abstraction from hydrosilanes of type Me_2ArSiH with a carborane-based trityl salt tends to form the trimethylsilylium ion, whereas hydrosilanes of type MeAr_2SiH with a bulky aryl substituent favor triarylsilylium ion generation.

Mechanism of the substituent redistribution reaction with Me_2PhSiH

To gain insight into the reaction mechanism and to understand why the treatment of Me_2PhSiH with $\text{Ph}_3\text{C}^+[\text{CHB}_{11}\text{H}_5\text{Br}_6]^-$ exclusively gives $\text{Me}_3\text{Si}^+[\text{CHB}_{11}\text{H}_5\text{Br}_6]^-$, we constructed a complete reaction energy profile using DFT calculations at the M06/cc-pVTZ(-f)//6-31G** level of theory (Fig. 3; see the ESI† for details of the computational method).²⁰ The hydride abstraction from Me_2PhSiH with $\text{Ph}_3\text{C}^+[\text{CHB}_{11}\text{H}_5\text{Br}_6]^-$ was found to have a barrier of $15.5\text{ kcal mol}^{-1}$ and is therefore expected to occur rapidly at room temperature (not shown). In the condensed phase, the resulting silylium ion Me_2PhSi^+ (**6A**), which is located at a relative free energy of 6.5 kcal mol^{-1} , is stabilized through coordination by the solvent, another hydrosilane molecule, or by the counteranion (see the ESI† for a comparison of the association energies).^{8e,21} Coordination of one of the bromine atoms of the carborane counteranion to the silicon cation results in the highest binding energy, and the resulting ion pair **6A'** is predicted to be at a relative free energy of $-24.1\text{ kcal mol}^{-1}$. Silylium ion **6A** can also interact with another equivalent of Me_2PhSiH to form hydride-bridged adduct **7A**,²¹

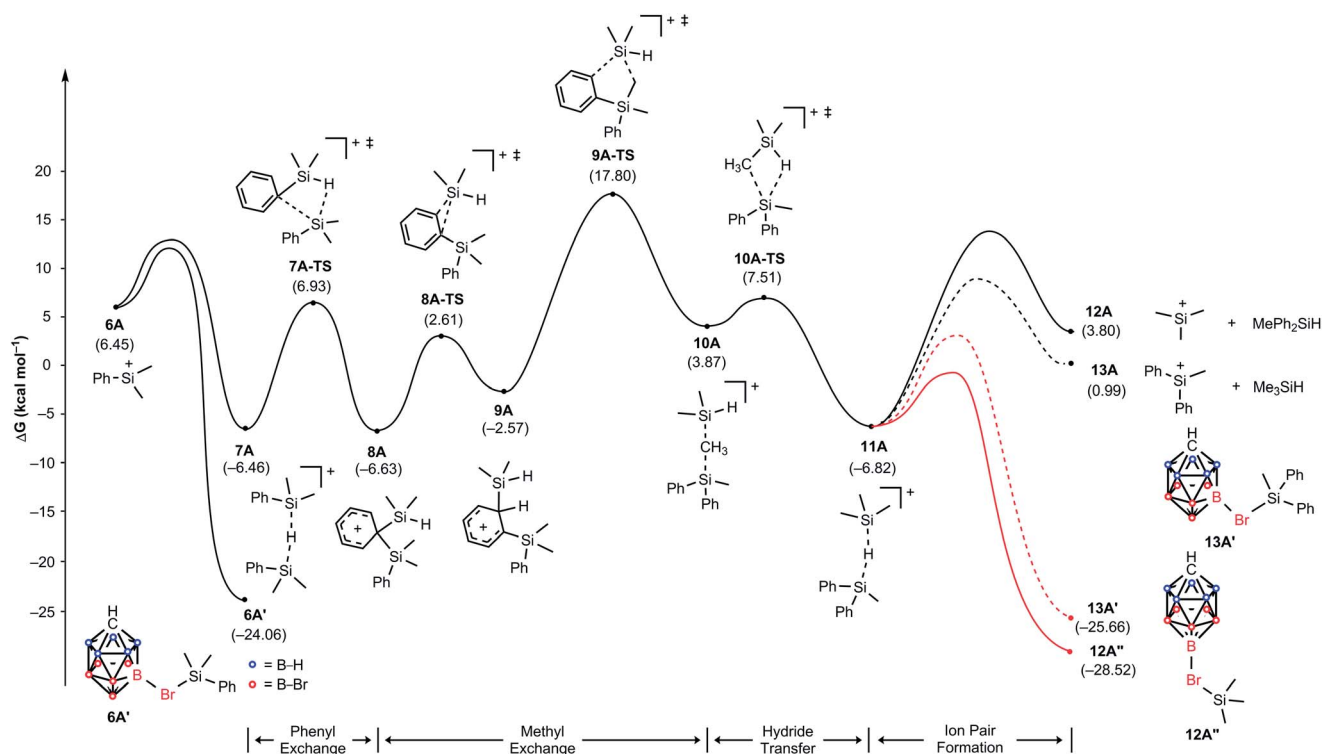


Fig. 3 Energy (kcal mol^{-1}) profile of the substituent redistribution in the reaction of Me_2PhSiH (**1A**) with $\text{Ph}_3\text{C}^+[\text{CHB}_{11}\text{H}_5\text{Br}_6]^-$ (**2A**). The energies are relative to the starting materials **1A** and **2A**.



located at $-6.5 \text{ kcal mol}^{-1}$. Note that these energies are not adjusted for the different concentrations of the components and assume normal conditions. Given that Me_2PhSiH (**1A**) is present in excess, these normal energies suggest that adduct **7A** will be encountered easily in significant quantities.

Hydride-bridged adduct ion **7A** can undergo a phenyl group transfer to arrive at phenyl-bridged adduct **8A**^{7c,8b,22} via the four-centered transition state **7A-TS**, associated with a barrier of $13.4 \text{ kcal mol}^{-1}$. Surprisingly, the subsequent methyl group transfer does not proceed via another typical four-membered transition state.²³ Instead, our calculations suggest that 1,2-migration of the silicon group in **8A** occurs via the low barrier transition state **8A-TS**, leading to *ortho*-disilylated arenium ion **9A**. This seemingly unfavorable intermediate is only $4.1 \text{ kcal mol}^{-1}$ higher in energy than arenium ion **8A**. Finally, **9A** facilitates the exchange of one methyl group, passing through five-centered transition state **9A-TS** with an overall barrier of $24.3 \text{ kcal mol}^{-1}$ relative to **7A**. This energetically most demanding reaction step forms methonium ion **10A**, which is metastable and rapidly rearranges to hydride-bridged adduct **11A** via low barrier transition state **10A-TS**. The hydrosilane-stabilized silylium ions **7A** and **11A** are almost isoenergetic ($\Delta G = 0.4 \text{ kcal mol}^{-1}$), suggesting that both structures coexist in equilibrium. The formal dissociation of **11A** gives either Me_3Si^+ or MePh_2Si^+ , the former being calculated to be $2.8 \text{ kcal mol}^{-1}$ higher in energy. However, coordination by the carborane anion changes the energy landscape decisively, as ion pair formation reverses the energy ordering. $\text{Me}_3\text{Si}^+[\text{CHB}_{11}\text{H}_5\text{Br}_6]^-$ (**12A''**), which is located at $-28.5 \text{ kcal mol}^{-1}$, is $2.9 \text{ kcal mol}^{-1}$ lower in energy than $\text{MePh}_2\text{Si}^+[\text{CHB}_{11}\text{H}_5\text{Br}_6]^-$ (**13A'**) and also $4.5 \text{ kcal mol}^{-1}$ more stable than $\text{Me}_2\text{PhSi}^+[\text{CHB}_{11}\text{H}_5\text{Br}_6]^-$ (**6A'**), thus predicting the silylium salt **12A''** as the major product of the substituent redistribution reaction.

It should be noted that silylium ions are significantly more stabilized by coordination of the carborane counteranion than by formation of solvent adducts such as $\text{R}_3\text{Si}(\text{toluene})^+[\text{CHB}_{11}\text{H}_5\text{Br}_6]^-$. Moreover, the energy differences between these arenium ions are small, predicting a mixture of different silylium ions in the absence of the carborane counteranion (see the ESI† for details).²⁴ This result was supported by independent control experiments (Scheme 2). The hydride abstraction from Me_2PhSiH with borate-based trityl salt $\text{Ph}_3\text{C}^+[\text{B}(\text{C}_6\text{F}_5)_4]^-$ was repeated but stopped after stirring for 10 min in toluene (*cf.* Table 1, entry 5). NMR spectroscopic analysis of the polar phase in *o*- $\text{Cl}_2\text{C}_6\text{D}_4$ revealed the formation of a mixture of $\text{Me}_3\text{Si}^+[\text{B}(\text{C}_6\text{F}_5)_4]^-$ and $\text{Me}_2\text{PhSi}^+[\text{B}(\text{C}_6\text{F}_5)_4]^-$ in a ratio of $\sim 51 : 49$ along with small amounts of byproducts arising from counteranion

decomposition. In contrast, stopping the reaction of Me_2PhSiH with $\text{Ph}_3\text{C}^+[\text{CHB}_{11}\text{H}_5\text{Br}_6]^-$ after stirring for 10 min in toluene furnished $\text{Me}_3\text{Si}^+[\text{CHB}_{11}\text{H}_5\text{Br}_6]^-$ as the major product along with only small amounts of unscrambled $\text{Me}_2\text{PhSi}^+[\text{CHB}_{11}\text{H}_5\text{Br}_6]^-$ (ratio $\sim 84 : 16$). In both reactions, full conversion of the trityl salt was observed.

As shown in Fig. 4, the silylium ions can be bound either to the apical or one of the equatorial bromine atoms of the carborane counteranion, with a slight preference of $1.1 \text{ kcal mol}^{-1}$ for the apical position in $\text{Me}_3\text{Si}^+[\text{CHB}_{11}\text{H}_5\text{Br}_6]^-$ (**12A''**). This result is in contrast to the molecular structure in the solid state, which shows the equatorial isomer (*cf.* Fig. 2). We speculate that either packing effects or a statistical preference for the equatorial isomer is the reason for this discrepancy. Notably, the equatorial isomer **12A'** is still $1.8 \text{ kcal mol}^{-1}$ lower in energy than the equatorial isomer of $\text{MePh}_2\text{Si}^+[\text{CHB}_{11}\text{H}_5\text{Br}_6]^-$ (**13A'**). The higher ion pairing energy in **12A'** can be ascribed to the low steric demand of Me_3Si^+ , leading to a closer carborane coordination and to attractive van der Waals interactions between the methyl moieties and the carborane anion. Especially in the apical position, the methyl functionality can interact with the highly polarizable bromine atoms. In contrast, the molecular fit of the sterically more demanding silylium ions Me_2PhSi^+ (**6A**) and MePh_2Si^+ (**13A**) with the carborane counteranion is less

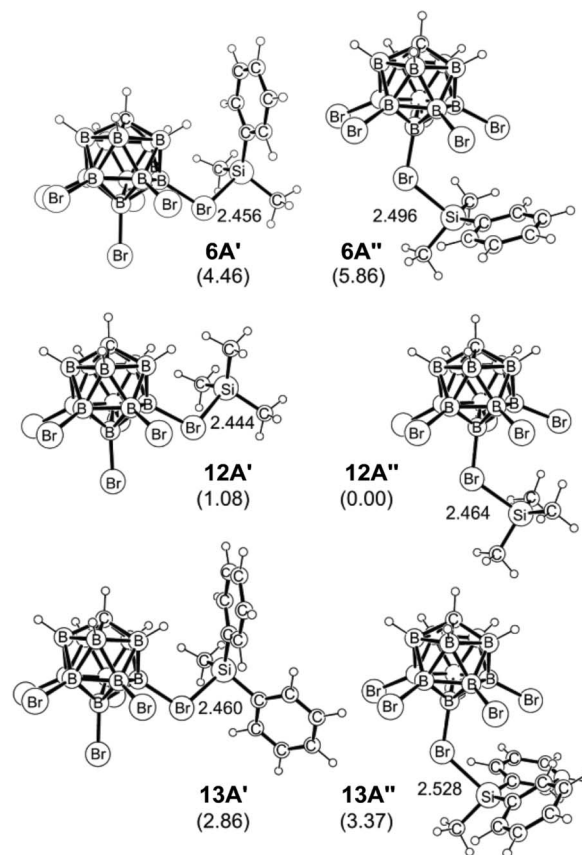
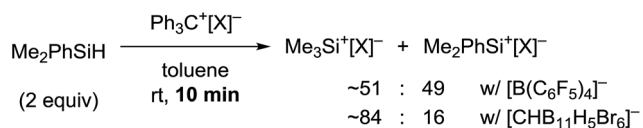


Fig. 4 Computed apical and equatorial isomers of $\text{Me}_2\text{PhSi}^+[\text{CHB}_{11}\text{H}_5\text{Br}_6]^-$ (top), $\text{Me}_3\text{Si}^+[\text{CHB}_{11}\text{H}_5\text{Br}_6]^-$ (middle) and $\text{MePh}_2\text{Si}^+[\text{CHB}_{11}\text{H}_5\text{Br}_6]^-$ (bottom). Si-Br bond lengths are given in Å and relative free energy differences (kcal mol^{-1}) are shown in parentheses.



tight, and the ion pairing is therefore slightly less favorable. This trend is reflected in the corresponding Si–Br bond lengths of these silylium carborane salts, which were computed to be shortest in both isomers of $\text{Me}_3\text{Si}^+[\text{CHB}_{11}\text{H}_5\text{Br}_6]^-$ (**12A'** and **12A''**). Hence, this ion pair is the most stable silylium salt despite the lack of stabilizing phenyl groups. Both isomers of $\text{Me}_2\text{PhSi}^+[\text{CHB}_{11}\text{H}_5\text{Br}_6]^-$ (**6A'** and **6A''**) are higher in energy than the corresponding $\text{MePh}_2\text{Si}^+[\text{CHB}_{11}\text{H}_5\text{Br}_6]^-$ (**13A'** and **13A''**), indicating that the stabilization of these silylium carborane salts is determined by a delicate balance of electronic and steric effects. It should also be noted here that the DFT optimized structures for $\text{Me}_3\text{Si}^+[\text{CHB}_{11}\text{H}_5\text{Br}_6]^-$ (**12A'**) and $\text{MePh}_2\text{Si}^+[\text{CHB}_{11}\text{H}_5\text{Br}_6]^-$ (**13A'**) are in good agreement with the corresponding molecular structures obtained by X-ray diffraction analysis (see the ESI† for details).

Mechanism of the substituent redistribution reaction with MePh_2SiH

To understand why the reaction of MePh_2SiH with $\text{Ph}_3\text{C}^+[\text{CHB}_{11}\text{H}_5\text{Br}_6]^-$ does not furnish $\text{Me}_3\text{Si}^+[\text{CHB}_{11}\text{H}_5\text{Br}_6]^-$, we constructed again a complete energy profile employing DFT simulations (Fig. 5). The initial hydride transfer of the hydrosilane to the trityl cation has a calculated barrier of $14.3 \text{ kcal mol}^{-1}$ (not shown), which is $1.2 \text{ kcal mol}^{-1}$ lower in energy compared to the case of Me_2PhSiH due to the slightly higher hydride donor strength of MePh_2SiH (see Table S1 in the

ESI† for details). The resulting silylium ion MePh_2Si^+ (**6B**) with a relative free energy of $0.8 \text{ kcal mol}^{-1}$ is almost isoenergetic to the reactant state. Adduct formation with another equivalent of MePh_2SiH affords hydrosilane-stabilized silylium ion **7B**, which undergoes a phenyl/methyl exchange reaction following a very similar reactivity pattern as described above, leading to scrambled hydride-bridged adduct **11B**. The transformation of **7B** to **11B** *via* intermediates **8B**, **9B**, and **10B** is again reversible, since **7B** and **11B** have similar free energies ($\Delta G = 0.7 \text{ kcal mol}^{-1}$). As before, the methyl group transfer *via* five-membered transition state **9B-TS** shows the highest barrier, which is $24.2 \text{ kcal mol}^{-1}$ relative to **7B**. In this equilibrium, unscrambled $\text{MePh}_2\text{Si}^+[\text{CHB}_{11}\text{H}_5\text{Br}_6]^-$ (**6B'**) with a relative free energy of $-25.9 \text{ kcal mol}^{-1}$ is predicted to be the major species, followed by scrambled $\text{Me}_2\text{PhSi}^+[\text{CHB}_{11}\text{H}_5\text{Br}_6]^-$ (**12B'**) and $\text{Ph}_3\text{Si}^+[\text{CHB}_{11}\text{H}_5\text{Br}_6]^-$ (**13B''**), which are basically isoenergetic at $-24.6 \text{ kcal mol}^{-1}$ and $-24.7 \text{ kcal mol}^{-1}$, respectively. This finding is in good agreement with the experimental observation of unscrambled $\text{MePh}_2\text{Si}^+[\text{CHB}_{11}\text{H}_5\text{Br}_6]^-$ being the main product of the reaction (*cf.* Table 1, entry 4).²⁵

Our calculations suggest that a subsequent methyl exchange reaction leading to Me_3Si^+ is unlikely (**11B** \rightarrow **18B**, gray energy profile in Fig. 5). The transition state for this methyl group transfer, **16B-TS**, is located $26.7 \text{ kcal mol}^{-1}$ relative to **11B**, which is $1.8 \text{ kcal mol}^{-1}$ higher in energy than the barrier of the backward reaction *via* transition state **9B-TS**. Consequently, the

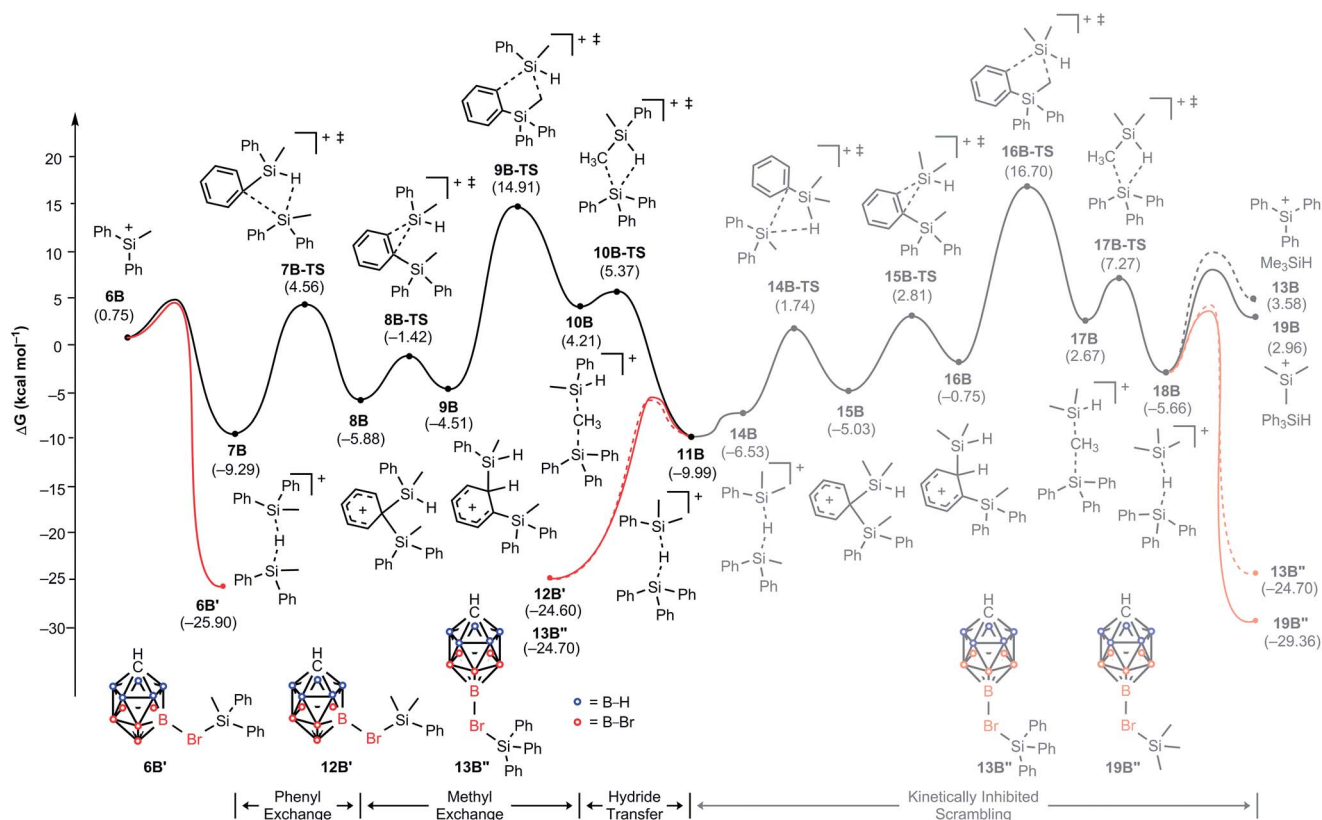


Fig. 5 Energy (kcal mol^{-1}) profile of the substituent redistribution in the reaction of MePh_2SiH (**1A**) with $\text{Ph}_3\text{C}^+[\text{CHB}_{11}\text{H}_5\text{Br}_6]^-$ (**2B**). The energies are relative to the starting materials **1B** and **2B**.

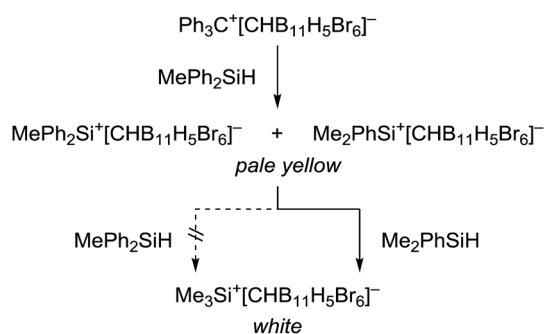


reaction of MePh_2SiH with $\text{Ph}_3\text{C}^+[\text{CHB}_{11}\text{H}_5\text{Br}_6]^-$ stops at the above-mentioned mixture of silicon cations rather than undergoing exhaustive substituent redistribution to furnish low energy $\text{Me}_3\text{Si}^+[\text{CHB}_{11}\text{H}_5\text{Br}_6]^-$.

This kinetic inhibition was further proven by another mechanistic control experiment (Scheme 3). When a mixture of $\text{Ph}_3\text{C}^+[\text{CHB}_{11}\text{H}_5\text{Br}_6]^-$ and MePh_2SiH in toluene was stirred overnight at room temperature, a pale yellow suspension was obtained, which is characteristic of silylium ions with aromatic substituents (*cf.* Table 1, entry 4). Addition of less bulky $\text{Me}_2\text{-PhSiH}$ to this mixture resulted in a quick decolorization and formation of a white suspension. NMR spectroscopic analysis of the solid now confirmed exclusive formation of $\text{Me}_3\text{Si}^+[\text{CHB}_{11}\text{H}_5\text{Br}_6]^-$.

Scope of the substituent redistribution reaction

The hydride abstraction from various dialkyl(phenyl)silanes with $\text{Ph}_3\text{C}^+[\text{CHB}_{11}\text{H}_5\text{Br}_6]^-$ finally revealed that the redistribution reaction is not restricted to methyl groups (Table 2). Although Et_2PhSiH reacted much slower compared to $\text{Me}_2\text{-PhSiH}$, exclusive formation of trialkylsilylium ion $\text{Et}_3\text{-Si}^+[\text{CHB}_{11}\text{H}_5\text{Br}_6]^-$ was observed (entries 1 and 2). Employing more bulky iPr_2PhSiH led to clean generation of unscrambled dialkyl(aryl)silylium ion $\text{iPr}_2\text{PhSi}^+[\text{CHB}_{11}\text{H}_5\text{Br}_6]^-$, as verified by X-ray crystallography (entry 3; see the ESI† for the molecular



Scheme 3 Probing the kinetic inhibition in the substituent redistribution reaction with MePh_2SiH .

Table 2 Silylium ion generation from hydrosilanes of type R_2PhSiH

R_2PhSiH (2 equiv)	$\text{Ph}_3\text{C}^+[\text{CHB}_{11}\text{H}_5\text{Br}_6]^-$ toluene rt, overnight	$\text{R}_3\text{Si}^+[\text{CHB}_{11}\text{H}_5\text{Br}_6]^-$ or $\text{R}_2\text{PhSi}^+[\text{CHB}_{11}\text{H}_5\text{Br}_6]^-$	$\delta(^{29}\text{Si})^b$ [ppm]
Entry ^a	R	Si ⁺	
1	Me	Me_3Si^+	93
2 ^c	Et	Et_3Si^+	100
3	iPr	$\text{iPr}_2\text{PhSi}^+$	76
4	<i>t</i> Bu	— ^d	—

^a All reactions were performed according to GP 2. See the ESI for details.
^b Measured in *o*- $\text{Cl}_2\text{C}_6\text{D}_4$. ^c With 4 equiv. of Et_2PhSiH and 7 days reaction time. ^d No reaction; only $\text{Ph}_3\text{C}^+[\text{CHB}_{11}\text{H}_5\text{Br}_6]^-$ was recovered.

Table 3 Silylium ion generation from hydrosilanes of type Me_2RSiH

Me_2RSiH (2 equiv)	$\text{Ph}_3\text{C}^+[\text{CHB}_{11}\text{H}_5\text{Br}_6]^-$ toluene rt, overnight	$\text{Me}_3\text{Si}^+[\text{CHB}_{11}\text{H}_5\text{Br}_6]^-$ or $\text{Me}_2\text{RSi}^+[\text{CHB}_{11}\text{H}_5\text{Br}_6]^-$	$\delta(^{29}\text{Si})^b$ [ppm]
Entry ^a	R	Si ⁺	
1	Ph	Me_3Si^+	93
2	Bn	Me_3Si^+	93
3	<i>t</i> Bu	$\text{Me}_2\text{tBuSi}^+$	98

^a All reactions were performed according to GP 2. See the ESI for details.
^b Measured in *o*- $\text{Cl}_2\text{C}_6\text{D}_4$.

structure of $\text{iPr}_2\text{PhSi}^+[\text{CHB}_{11}\text{H}_5\text{Br}_6]^-$.¹⁵ These results are in accordance with our calculations, predicting high energy barriers for the transfer of bulky alkyl groups. Sterically even more shielded *t*Bu₂PhSiH then completely thwarted the hydride abstraction, and only the trityl salt was recovered from the reaction mixture (entry 4).

To investigate whether the phenyl group in Me_2PhSiH can be replaced by other 'leaving groups', we also tested a benzyl and an alkyl substituent in Me_2RSiH (Table 3). As in the case of Me_2PhSiH (entry 1), clean formation of $\text{Me}_3\text{Si}^+[\text{CHB}_{11}\text{H}_5\text{Br}_6]^-$ was observed with Me_2BnSiH (entry 2), showing that the phenyl group is not essential for the exchange process. In contrast, the bulky *tert*-butyl group in Me_2tBuSiH completely prevented substituent redistribution, and silylium ion $\text{Me}_2\text{tBuSi}^+[\text{CHB}_{11}\text{H}_5\text{Br}_6]^-$ was formed as the only product (entry 3). This result again demonstrates that the intermolecular substituent exchange reaction is sensitive towards sterically demanding alkyl groups (*cf.* entry 3 in Table 2).

Conclusion

It has been known for decades that silylium ions can undergo redistribution reactions of their substituents.⁸ The present combined experimental and detailed computational study finally provides a full mechanistic picture of this phenomenon. The mechanism involves a series of phenyl and alkyl exchange reactions, the latter being calculated to be the energetically most demanding steps. While the transfer of phenyl groups proceeds *via* common four-centered transition states, the corresponding alkyl exchange was found to pass through unusual five-membered transition states. These are accessible after 1,2-silyl migration at the stage of the intermediate disilylated arenium ions.

Additionally, our DFT calculations revealed that the silicon cations are significantly more stabilized by ion pair formation with the carborane counteranion ($\text{R}_3\text{Si}^+[\text{CHB}_{11}\text{H}_5\text{Br}_6]^-$) than by formation of toluenium ($\text{R}_3\text{Si}(\text{toluene})^+[\text{CHB}_{11}\text{H}_5\text{Br}_6]^-$) or hydrosilane-stabilized silylium ions ($[\text{R}_3\text{Si}-\text{H}-\text{SiR}_3]^+[\text{CHB}_{11}\text{H}_5\text{Br}_6]^-$). More importantly, purely aliphatic silylium carboranes with small substituents, *i.e.*, methyl or ethyl groups, were found to be distinctly lower in energy than the corresponding mixed aliphatic/aromatic or purely aromatic silylium ion pairs as



a result of stronger attractive interactions ($\Delta G \geq 2.9$ kcal mol⁻¹ for R = Me). These energy differences account for the highly selective formation of Me₃Si⁺[CHB₁₁H₅Br₆]⁻ and Et₃Si⁺[CHB₁₁H₅Br₆]⁻ from the reaction of the corresponding hydrosilanes R₂PhSiH (R = Me, Et) with Ph₃C⁺[CHB₁₁H₅Br₆]⁻ under thermodynamic control.

The phenyl group in Me₂PhSiH turned out to be replaceable by other 'leaving groups', such as a benzyl or even a sterically demanding C₆Me₅ group. However, two alkyl groups must be preinstalled in the hydrosilane starting material to steer the reaction towards formation of Me₃Si⁺[CHB₁₁H₅Br₆]⁻. In contrast, hydride abstraction from MePh₂SiH with only one alkyl substituent leads to a mixture of different silylium ions, as exhaustive scrambling to Me₃Si⁺ is kinetically inhibited. Exchanging the phenyl groups in MePh₂SiH by 2,6-disubstituted aryl groups (e.g. C₆Me₅) eventually provides access to sterically congested triarylsilylium ions, as previously demonstrated by Müller and co-workers.¹⁰

These general trends provide a solid foundation for the mechanistic understanding of the substituent redistribution of silylium ions, thereby enabling the prediction of the outcome of these exchange reactions. Thus, this process can be used as a reliable synthetic route not only to triaryl- but also to trialkylsilylium ions by deliberate choice of the hydrosilane and counteranion of the trityl salt.

Conflicts of interest

There are no conflicts to declare.

Acknowledgements

L. O. thanks the Fonds der Chemischen Industrie for a predoctoral fellowship (2015–2017), and M. O. is indebted to the Einstein Foundation (Berlin) for an endowed professorship. B. P. and M.-H. B. are grateful for the financial support (IBS-R10-D1) from the Institute for Basic Science. DFT calculations were performed using the high performance computing facility located on the KAIST campus.

Notes and references

- For general reviews of silylium ion chemistry, see: (a) V. Y. Lee and A. Sekiguchi, in *Organosilicon Compounds*, ed. V. Y. Lee, Academic Press, Oxford, 2017, vol. 1, pp. 197–230; (b) T. Müller, in *Structure and Bonding*, ed. D. Scheschkewitz, Springer, Berlin, 2014, vol. 155, pp. 107–162; (c) T. Müller, in *Science of Synthesis Knowledge Updates 2013/3*, ed. M. Oestreich, Thieme, Stuttgart, 2013, pp. 1–42.
- For silylium ions in catalysis, see: (a) H. F. T. Klare, *ACS Catal.*, 2017, 7, 6999–7002; (b) A. Schulz and A. Villinger, *Angew. Chem., Int. Ed.*, 2012, 51, 4526–4528; (c) H. F. T. Klare and M. Oestreich, *Dalton Trans.*, 2010, 39, 9176–9184.
- (a) P. D. Bartlett, F. E. Condon and A. Schneider, *J. Am. Chem. Soc.*, 1944, 66, 1531–1539; (b) J. Y. Corey and R. West, *J. Am. Chem. Soc.*, 1963, 85, 2430–2433; (c) J. Y. Corey, *J. Am. Chem. Soc.*, 1975, 97, 3237–3238.
- For recent reviews of weakly coordinating anions, see: (a) I. M. Riddlestone, A. Kraft, J. Schaefer and I. Krossing, *Angew. Chem., Int. Ed.*, 2018, 57, DOI: 10.1002/anie.201710782; (b) T. A. Engesser, M. R. Lichtenthaler, M. Schleep and I. Krossing, *Chem. Soc. Rev.*, 2016, 45, 789–899.
- For further strategies to generate silylium ions, see: (a) J. B. Lambert, Y. Zhao, H. Wu, W. C. Tse and B. Kuhlmann, *J. Am. Chem. Soc.*, 1999, 121, 5001–5008 (allyl-leaving-group approach); (b) M. J. MacLachlan, S. C. Bourke, A. J. Lough and I. Manners, *J. Am. Chem. Soc.*, 2000, 122, 2126–2127 (ring-opening protonolysis); (c) A. Schäfer, M. Reißmann, A. Schäfer, M. Schmidtman and T. Müller, *Chem.–Eur. J.*, 2014, 20, 9381–9386 (silylene protonation); (d) A. Simonneau, T. Biberger and M. Oestreich, *Organometallics*, 2015, 34, 3927–3929 (cyclohexadienyl-leaving-group approach); (e) Q.-A. Chen, H. F. T. Klare and M. Oestreich, *J. Am. Chem. Soc.*, 2016, 138, 7868–7871 (hydrosilane protonation).
- For a review of substituent redistribution reactions at silicon, see: D. R. Weyenberg, L. G. Mahone and W. H. Atwell, *Ann. N. Y. Acad. Sci.*, 1969, 159, 38–55.
- For Lewis acid-catalyzed substituent redistribution reactions of hydrosilanes, see: (a) J. L. Speier and R. E. Zimmerman, *J. Am. Chem. Soc.*, 1955, 77, 6395–6396; (b) M. Khandelwal and R. J. Wehmschulte, *Angew. Chem., Int. Ed.*, 2012, 51, 7323–7326; (c) A. Feigl, I. Chiorescu, K. Deller, S. U. H. Heidsieck, M. R. Buchner, V. Karttunen, A. Bockholt, A. Genest, N. Rösch and B. Rieger, *Chem.–Eur. J.*, 2013, 19, 12526–12536; (d) R. J. Wehmschulte, M. Saleh and D. R. Powell, *Organometallics*, 2013, 32, 6812–6819; (e) R. Labbow, F. Reiß, A. Schulz and A. Villinger, *Organometallics*, 2014, 33, 3223–3226; (f) J. Chen and E. Y.-X. Chen, *Angew. Chem., Int. Ed.*, 2015, 54, 6842–6846; (g) Y. Ma, L. Zhang, Y. Luo, M. Nishiura and Z. Hou, *J. Am. Chem. Soc.*, 2017, 139, 12434–12437.
- For substituent redistribution reactions of silicon cations, see: (a) C. Eaborn, P. D. Lickiss, S. T. Najim and W. A. Stańczyk, *J. Chem. Soc., Chem. Commun.*, 1987, 1461–1462; (b) N. Choi, P. D. Lickiss, M. McPartlin, P. C. Masangane and G. L. Veneziani, *Chem. Commun.*, 2005, 6023–6025; (c) N. Lühmann, H. Hirao, S. Shaik and T. Müller, *Organometallics*, 2011, 30, 4087–4096; (d) K. Múther, P. Hrobárik, V. Hrobáriková, M. Kaupp and M. Oestreich, *Chem.–Eur. J.*, 2013, 19, 16579–16594; (e) S. J. Connelly, W. Kaminsky and D. M. Heinekey, *Organometallics*, 2013, 32, 7478–7481; (f) Ref. 7e; (g) L. Albers, S. Rathjen, J. Baumgartner, C. Marschner and T. Müller, *J. Am. Chem. Soc.*, 2016, 138, 6886–6892.
- For seminal reports, see: (a) J. B. Lambert, S. Zhang, C. L. Stern and J. C. Huffman, *Science*, 1993, 260, 1917–1918; (b) C. A. Reed, Z. Xie, R. Bau and A. Benesi, *Science*, 1993, 262, 402–404.
- (a) A. Schäfer, M. Reißmann, A. Schäfer, W. Saak, D. Haase and T. Müller, *Angew. Chem., Int. Ed.*, 2011, 50, 12636–



- 12638; (b) A. Schäfer, M. Reißmann, S. Jung, A. Schäfer, W. Saak, E. Brendler and T. Müller, *Organometallics*, 2013, **32**, 4713–4722.
- 11 (a) J. B. Lambert and Y. Zhao, *Angew. Chem., Int. Ed. Engl.*, 1997, **36**, 400–401; (b) K.-C. Kim, C. A. Reed, D. W. Elliot, L. J. Mueller, F. Tham, L. Lin and J. B. Lambert, *Science*, 2002, **297**, 825–827; (c) J. B. Lambert and L. Lin, *J. Org. Chem.*, 2001, **66**, 8537–8539.
- 12 Hydride abstraction from MePh_2SiH with $\text{Ph}_3\text{C}^+[\text{B}(\text{C}_6\text{F}_5)_4]^-$ was reported as a clean reaction: J. B. Lambert, S. Zhang and S. M. Ciro, *Organometallics*, 1994, **13**, 2430–2443. However, this result could not be reproduced by Müller (*cf.* ref. 10b) and us.
- 13 (a) C. A. Reed, *Acc. Chem. Res.*, 1998, **31**, 133–139; (b) C. A. Reed, *Acc. Chem. Res.*, 2010, **43**, 121–128.
- 14 For the synthesis and crystallographic characterization of related trimethylsilylium salts, see: (a) $\text{Me}_3\text{Si}^+[\text{CRB}_{11}\text{F}_{11}]^-$ (R = H, Et): T. Küppers, E. Bernhardt, R. Eujen, H. Willner and C. W. Lehmann, *Angew. Chem., Int. Ed.*, 2007, **46**, 6346–6349; (b) $\text{Me}_3\text{Si}(\text{arene})^+[\text{B}(\text{C}_6\text{F}_5)_4]^-$: M. F. Ibad, P. Langer, A. Schulz and A. Villinger, *J. Am. Chem. Soc.*, 2011, **133**, 21016–21027.
- 15 CCDC 1818576 for $\text{Me}_3\text{Si}^+[\text{CHB}_{11}\text{H}_5\text{Br}_6]^-$, CCDC 1818582 for $\text{MePh}_2\text{Si}^+[\text{CHB}_{11}\text{H}_5\text{Br}_6]^-$, and CCDC 1818581 for $\text{iPr}_2\text{PhSi}^+[\text{CHB}_{11}\text{H}_5\text{Br}_6]^-$ contain the supplementary crystallographic data for this paper.†
- 16 Z. Xie, R. Bau, A. Benesi and C. A. Reed, *Organometallics*, 1995, **14**, 3933–3941.
- 17 The decomposition of the $[\text{B}(\text{C}_6\text{F}_5)_4]^-$ counteranion is likely to proceed *via* an $\text{S}_{\text{E}}\text{Ar}$ reaction of the formed silylium ions with the borate. The formation of $\text{B}(\text{C}_6\text{F}_5)_3$ was verified by ^{19}F NMR spectroscopic analysis, and GC-MS analysis revealed formation of several silanes containing a C_6F_5 unit.
- 18 The generated silylium ions were converted to the corresponding fluorosilanes using $(\text{C}_6\text{F}_5)_3\text{PF}_2$ (1.0 equiv.), thereby facilitating product characterization by both NMR spectroscopic and GC-MS analysis. For the preparation of $(\text{C}_6\text{F}_5)_3\text{PF}_2$, see: C. B. Caputo, L. J. Hounjet, R. Dobrovetsky and D. W. Stephan, *Science*, 2013, **341**, 1374–1377.
- 19 Small amounts of the triarylsilylium ion $(\text{C}_6\text{Me}_5)_3\text{Si}^+[\text{CHB}_{11}\text{H}_5\text{Br}_6]^-$ were also detected (*cf.* ref. 10).
- 20 The mechanism of intermolecular substituent exchange reactions at related ferrocene-stabilized silylium ions had already been studied by quantum-chemical analyses (*cf.* ref. 8d). However, the calculated barriers for the transition states were relatively high. For the calculated mechanism of an intramolecular substituent exchange reaction at a silicon cation with a rigid naphthalene-1,8-diyl backbone, see: ref. 8c.
- 21 (a) S. P. Hoffmann, T. Kato, F. S. Tham and C. A. Reed, *Chem. Commun.*, 2006, 767–769; (b) M. Nava and C. A. Reed, *Organometallics*, 2011, **30**, 4798–4800.
- 22 R. Meyer, K. Werner and T. Müller, *Chem.–Eur. J.*, 2002, **8**, 1163–1171.
- 23 We were not able to locate a four-centered transition state from **8A** to directly arrive at **10A**. See Fig. S67 in the ESI† for geometric scan calculations.
- 24 $\text{Me}_3\text{Si}(\text{toluene})^+[\text{CHB}_{11}\text{H}_5\text{Br}_6]^-$ was calculated to be only 0.7 kcal mol $^{-1}$ lower in energy than $\text{MePh}_2\text{Si}(\text{toluene})^+[\text{CHB}_{11}\text{H}_5\text{Br}_6]^-$ (see the ESI† for details).
- 25 Although our calculations predict formation of small amounts of $\text{Ph}_3\text{Si}^+[\text{CHB}_{11}\text{H}_5\text{Br}_6]^-$ in the reaction of MePh_2SiH with $\text{Ph}_3\text{C}^+[\text{CHB}_{11}\text{H}_5\text{Br}_6]^-$, we were not able to detect this silylium ion by $^1\text{H}/^{29}\text{Si}$ HMQC NMR spectroscopy.

